European Review for Medical and Pharmacological Sciences 2020; 24: 2173-2180

Effect of lncRNA AK125437 on postmenopausal osteoporosis rats *via* MAPK pathway

H. WANG[1], Y.-K. LI[2], M. CUI[1], L.-H. LIU[1], L.-M. ZHAO[2], X.-M. WANG[3]

[1]Department of Orthopedics, Jinan Traditional Chinese Medicine Hospital, Jinan, China
[2]Department of Public Health, Fourth People's Hospital of Jinan, Jinan, China
[3]Department of Orthopedics, Fourth People's Hospital of Jinan, Jinan, China

Hui Wang and Yunkai Li contributed equally to the work

Abstract. – OBJECTIVE: The aim of this study was to explore the effect of long non-coding ribonucleic acid (lncRNA) AK125437 on rats with postmenopausal osteoporosis via the mitogen-activated protein kinase (MAPK) pathway.

MATERIALS AND METHODS: A total of 36 Sprague-Dawley rats were randomly divided into three groups, including normal group, model group, and an inhibitor group, with 12 rats in each group. Only ovaries were exposed in normal group. The postmenopausal osteoporosis model was established in model group. Meanwhile, the intervention was performed with inhibitor for 3 months after modeling in inhibitor group, followed by sampling. The expression of receptor activator of nuclear factor kappa-B ligand (RANKL) was detected via immunohistochemistry. The protein expression level of phosphorylated p38 (p-p38) MAPK was determined via Western blotting (WB). Furthermore, the expression level of lncRNA AK125437 and the content of serum estradiol were determined via quantitative Polymerase Chain Reaction (qPCR) and enzyme-linked immunosorbent assay (ELISA), respectively. In addition, bone mineral density was measured using dual-energy X-ray bone mineral absorptiometer.

RESULTS: Immunohistochemistry results indicated that model group and inhibitor group had notably up-regulated positive expression level of RANKL than normal group ($p<0.05$), which was remarkably lower in inhibitor group than model group ($p<0.05$). Western blot results showed that compared with normal group, the protein expression level of p-p38 MAPK was substantially elevated in model and inhibitor groups ($p<0.05$). Meanwhile, the protein expression level of p-p38 MAPK was markedly lower in inhibitor group than that in model group ($p<0.05$). According to qPCR results, the expression level of lncRNA AK125437 was significantly up-regulated in both model group and inhibitor group compared with normal group, showing statistically significant differences ($p<0.05$). However, no significant differences were observed between model group and inhibitor group ($p>0.05$). ELISA results revealed that model group and inhibitor group had markedly lower estradiol content than normal group ($p<0.05$). There was no statistically significant difference in the content of estradiol between the two groups ($p>0.05$). According to the measurement results of bone mineral density, compared with normal group, bone mineral density was notably lower in model group and inhibitor group ($p<0.05$). Furthermore, it was markedly higher in inhibitor group than that of model group ($p<0.05$).

CONCLUSIONS: LncRNA AK125437 affects the bone mineral density of rats with postmenopausal osteoporosis by activating the MAPK pathway.

Key Words:
Postmenopausal osteoporosis, MAPK signaling pathway, LncRNA.

Introduction

Postmenopausal osteoporosis is an important disease of the perimenopausal syndrome, which often occurs in postmenopausal women aged about 50 years old. It is characterized by high clinical morbidity rate and persistent pain[1,2]. The onset of postmenopausal osteoporosis is closely related to the fact that the weakening of ovarian function due to ovary degeneration may lead to metabolic disorders of the endocrine system. This may eventually affect bone metabolism. As a major perimenopausal syndrome, postmenopausal osteoporosis tends to cause persistent pain, susceptibility to fractures, as well as even disability and death[3,4]. Hence, it is urgent to explore the pathogenesis and related treatments of postmenopausal osteoporosis.

Long non-coding ribonucleic acids (lncRNAs) have been confirmed to participate in multiple bio-

Corresponding Author: Ximing Wang, BM; e-mail: zhenhong961@163.com

logical processes, such as transcriptional regulation of genes, epigenetic modification, and protein translational modification. Meanwhile, lncRNAs play crucial regulatory roles in multiple diseases[5,6]. Currently, it is recognized that lncRNAs play important regulatory effects on bone metabolism-related signaling pathways. Meanwhile, they can regulate several pathways that are related to osteoblast, osteoclast differentiation, as well as calcium metabolism, thereby participating in the onset of osteoporosis. The p38 mitogen-activated protein kinase (MAPK) signaling pathway serves as an important regulator in abnormal bone metabolism in osteoporosis[7,8]. Once activated, this pathway promotes the proliferation and differentiation of osteoclasts, ultimately aggravating osteoporosis. Therefore, the aim of the present work was to investigate the influence of lncRNA AK125437 on rats with postmenopausal osteoporosis *via* the MAPK pathway. Furthermore, we aimed to elucidate the important role of lncRNA AK125437 and its mechanism of action in postmenopausal osteoporosis.

Materials and Methods

Laboratory Animals and Grouping

A total of 36 Sprague-Dawley rats weighing 220±20 g [Shanghai SLAC Laboratory Animal Co., Ltd., Shanghai, China, license No. SCXK (Hu) 2014-0003] were randomly assigned into three groups using a random number table, including normal group (n=12), model group (n=12), and inhibitor group (n=12). This research was approved by the Animal Ethics Committee of Jinan Traditional Chinese Medicine Hospital Animal Center.

Experimental Reagents and Instruments

Inhibitor: SB 203580 (Millipore, Billerica, MA, USA), primary antibodies: anti-receptor activator of nuclear factor kappa-B ligand (RANKL) antibody and anti-phosphorylated p38 (p-p38) MAPK antibody (Abcam, Cambridge, MA, USA), estradiol enzyme-linked immunosorbent assay (ELISA) kit (BOSTER Biological Technology Co., Ltd., Wuhan, China), AceQ quantitative polymerase chain reaction (qPCR) SYBR Green Master Mix kit and HiScript II Q RT SμperMix for qPCR [+genomic deoxyribonucleic acid (gDNA) wiper] kit (Vazyme Biotech, Nanjing, China), optical microscope (Leica DMI 4000B/DFC425C, Germany), fluorescence qPCR instrument (ABI 7500; Waltham, MA, USA) and Image-Pro image analysis system (Bio-Rad, Hercules, USA).

Modeling

After successful anesthetization *via* intraperitoneal injection of 7% chloral hydrate at a dose of 5 mL/kg, the specific operation procedure was performed as follows. First, the rats were fixed. Then, they were shaved with the rear of the 12th rib as the center. After disinfection, a 3 cm-long longitudinal incision was made to cut open and carefully strip off the skin and fascia, followed by exposure of the ovaries. Next, oviducts below the ovaries were ligated, and both ovaries were removed. Finally, after rinsing the incision, the skin was sutured and wrapped up.

Treatments in Each Group

In normal group, ovaries of rats were exposed, and the incision was sutured. To resect the ovaries, rats received routine postoperative care and diet without any treatment. In model group, after the establishment of postmenopausal osteoporosis model, the rats were routinely cared and fed for 3 months. Additionally, in inhibitor group, after the establishment of the postmenopausal osteoporosis model as mentioned above, the rats were given routine postoperative care and diet, followed by an intraperitoneal injection with SB203580 (100 mg/kg) daily. The intervention lasted for 3 months, and the samples were taken.

Sampling

Blood was first drawn from the abdominal aorta of all rats successfully anesthetized. Subsequently, 6 rats in each group were fixed with paraformaldehyde perfusion, followed by a collection of lumbar and femoral tissues. These tissues were then fixed in 4% paraformaldehyde at 4°C for 48 h, followed by preparation of paraffin-embedded tissue sections for immunohistochemistry, and hematoxylin-eosin (HE) staining. In addition, lumbar and femoral tissues were directly sampled from the remaining 6 rats in each group. These tissues were placed in Eppendorf (EP) tubes and were used for Western blotting (WB) and qPCR.

Immunohistochemistry

Pre-paraffin-embedded tissues were made into 5 μm-thick sections and placed in 42°C warm water After extending, mounting, and baking, the tissues were prepared into paraffin-embedded tissue sections. The sections were routinely de-paraffinized and dehydrated through soaking in xylene solution and gradient ethanol successively. Subsequently, the sections were immersed in citrate buffer and heated repeatedly using a mi-

crowave oven for 3 times (heating for 3 min and braising for 5 min per time) for complete antigen retrieval. After rinsing, the sections were added dropwise with endogenous peroxidase blocker. After reaction for 10 min, the sections were rinsed and sealed with goat serum for 20 min. After discarding the goat serum sealing solution, the tissue sections were incubated with anti-RANKL primary antibody (1:200) in a refrigerator at 4°C overnight. On the next day, the sections were incubated with the corresponding secondary antibody solution for 10 min. After fully rinsing, they were reacted with a streptavidin-peroxidase solution for 10 min. Color development was performed using diaminobenzidine (DAB). Finally, the nuclei were counterstained using hematoxylin, and the sections were sealed and observed.

Western Blotting (WB)

Lumbar and femoral tissues stored at ultralow temperature were added with lysis buffer. After bathing on ice for 1 h, the tissues were centrifuged at 14,000 g for 10 min. The concentration of extracted protein was quantified using the bicinchoninic acid method (BCA; Pierce, Rockford, IL, USA). To calculate the concentration of proteins, the absorbance was measured using a microplate reader, and the standard curve was plotted. Subsequently, protein samples were separated *via* dodecyl sulfate, sodium salt-polyacrylamide gel electrophoresis (SDS-PAGE) and transferred onto polyvinylidene difluoride (PVDF) membranes (Roche, Basel, Switzerland). After reaction with the sealing solution for 1.5 h, the membranes were incubated with anti-p-p38 MAPK primary antibody (1:1,000) overnight. On the next day, the membranes were incubated with the corresponding secondary antibody (1:1,000) at room temperature for 1 h. After rinsing, the sections were fully developed in the dark through reaction with a chemiluminescent reagent for 1 min.

Quantitative Polymerase Chain Reaction (QPCR)

Total RNA was first extracted and reversely transcribed into complementary DNA (cDNA) using a reverse transcription kit (20 μL). Specific reaction conditions were as follows: reaction at 51°C for 2 min, pre-degeneration at 96°C for 10 min, degeneration at 96°C for 10 s, and annealing at 60°C for 30 s, for a total of 40 cycles. Relative expression levels of messenger RNAs (mRNAs) were calculated. Glyceraldehyde-3-phosphate dehydrogenase (GAPDH) was used as an internal reference. Primer sequences used in this study were shown in Table I.

Determination of Bone Mineral Density

Femoral bone mineral density was measured by dual-energy X-ray bone mineral densitometer. Briefly, the femurs were fixed with paraformaldehyde. Then, the femurs were placed in the instrument, with the variable coefficient set as <1.0%.

ELISA

First, abdominal aortic blood was centrifuged at 14,000 g for 10 min, followed by the collection of the supernatant. The content of serum estradiol was measured according to the instructions of the ELISA kit.

Statistical Analysis

Statistical Product and Service Solutions (SPSS) 20.0 (SPSS, Chicago, IL, USA) software was used for all statistical analysis. Enumeration data were expressed as mean ± standard deviation (SD). The *t*-test was performed for data with normal distribution and homogeneity of variance. Corrected *t*-test was applied for data meeting normal distribution and heterogeneity of variance. A non-parametric test was used for data not in line with normal distribution and homogeneity of variance. One-way ANOVA test was applied to compare the differences among different groups,

Table I. Primer sequence.

Name	Primer sequence
lncRNA AK125437	Forward: 5′GACAGATGACACCTGTACAGATCA3' Reverse: 5′GTCTATTCATTACGCAGCGACAAGCC3'
RANKL	Forward: 5'TCCACCAAGAAGCTGAGCGAG3' Reverse: 5'GTCCAGCCCATGATGGTTCT3'
GAPDH	Forward: 5'ACGGCAAGTTCAACGGCACAG3' Reverse: 5'GAAGACGCCAGTAGACTCCACGAC3'

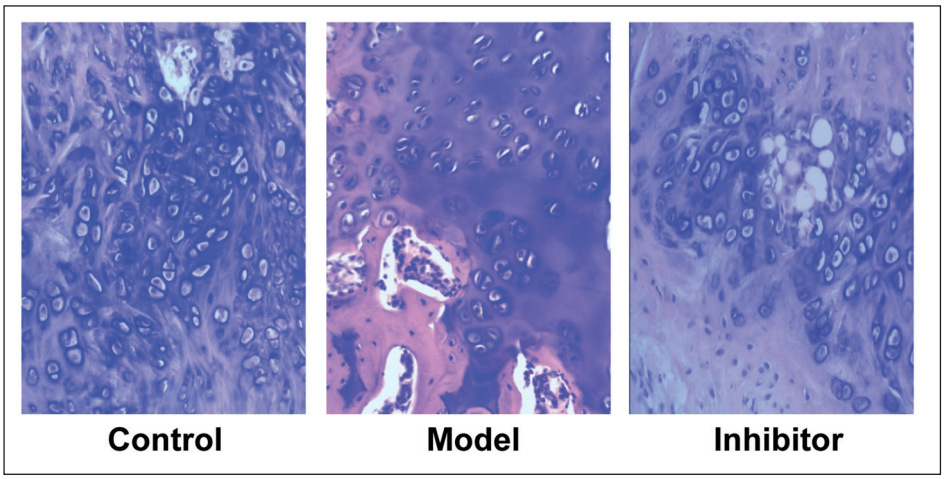

Figure 1. HE staining results (×200).

followed by Post-Hoc Test (Least Significant Difference). Ranked data and count data were subjected to rank-sum and chi-square tests, respectively. $p < 0.05$ was considered statistically significant.

Results

HE Staining

As shown in Figure 1, normal group exhibited bone tissues with regular morphology, intact structure, and plump and stout bone trabeculae. However, model group had bone tissues with less favorable morphology and incomplete structure, as well as visible rupture and fracture in some tissues. Besides, compared with model group, the bone tissue morphology was improved, wear was lighter, and trabeculae were denser in inhibitor group.

Immunohistochemistry

RANKL-positive cells were tan and there were fewer such cells in normal group, while more in model group (Figure 2). As shown in Figure 3, compared with normal group, the average optical density of cells with positively expressed RANKL was considerably up-regulated in model and inhibitor groups, showing statistically significant differences ($p<0.05$). However, it was markedly lower in inhibitor group than that of model group, with statistically significant differences ($p<0.05$).

Protein Expression of p-p38 MAPK Detected Via Western Blot

As shown in Figure 4, normal group showed a significantly lower protein expression level of p-p38 MAPK than model group ($p<0.05$). According to the statistical results (Figure 5), the relative protein expression level of p-p38 MAPK was substantially up-regulated in model and inhibitor

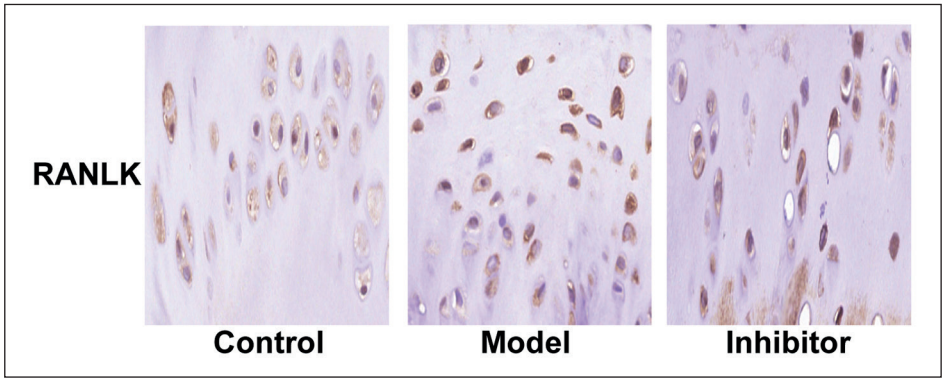

Figure 2. Immunohistochemistry detection results (×200).

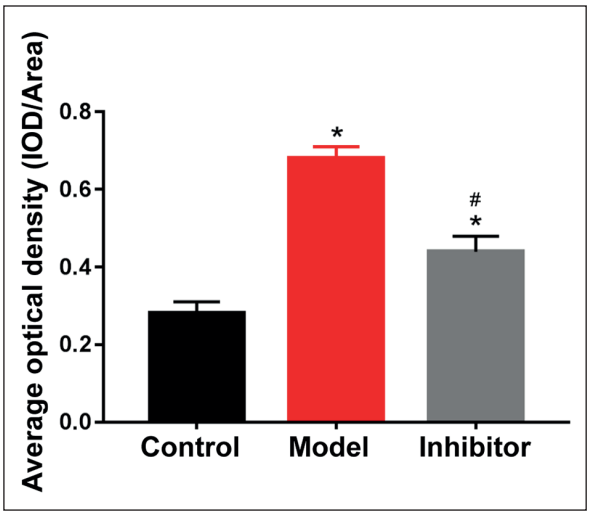

Figure 3. Average optical density of cells with positively expressed RANKL in each group. Note: *p<0.05 *vs.* normal group, and #p<0.05 *vs.* model group.

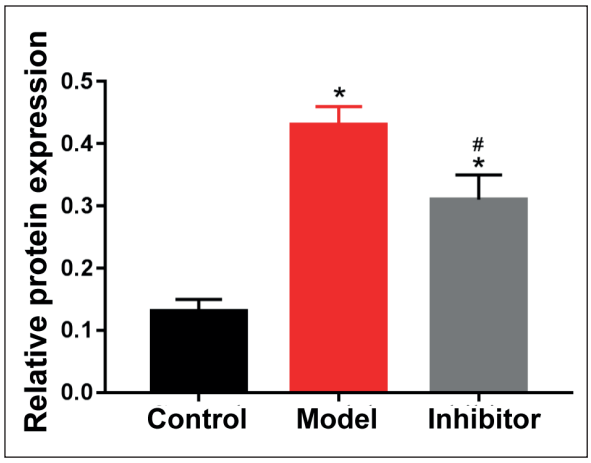

Figure 5. Protein expression level of p-p38 MAPK in each group. Note: *p<0.05 *vs.* normal group, and #p<0.05 *vs.* model group.

groups compared with normal group (p<0.05). Moreover, it was notably lower in inhibitor group than model group, showing statistically significant differences (p<0.05).

Expression Level of LncRNA AK125437 Determined Via qPCR

Compared with normal group, the relative mRNA expression level of lncRNA AK125437 was markedly elevated in model and inhibitor groups (p<0.05). However, no significant difference was observed between normal group and inhibitor group (p>0.05) (Figure 6).

ELISA

According to the results (Figure 7), model and inhibitor groups exhibited remarkably lower estradiol content than normal group, with statistically significant differences (p<0.05). However, there was no statistically significant difference in the content of estradiol between the two groups (p>0.05).

Bone Mineral Density

Compared with normal group, the bone mineral density was notably lower in both model group and inhibitor group, displaying statistically significant differences (p<0.05). However, it was remarkably higher in inhibitor group than that in model group (p<0.05) (Figure 8).

Discussion

Postmenopausal osteoporosis is now considered to occur in elderly postmenopausal women. Ovarian dysfunction causes inadequate estrogen secretion and affects bone metabolism, leading to bone loss to exceed the volume of bone formation. This may eventually increase bone fragility and damage osteoporosis in a long term[9,10]. The most common clinical symptoms of postmenopausal osteoporosis include persistent pain, malformation, and fracture induced by increased bone fragility, as well as damage to bone tissues.

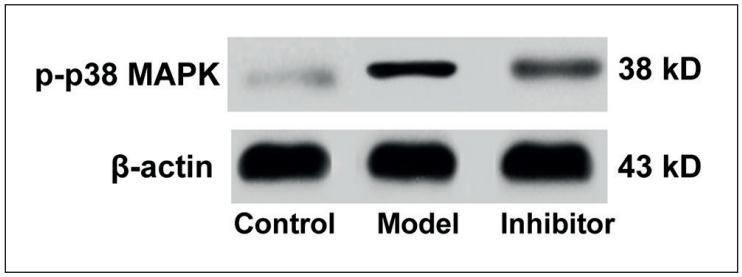

Figure 4. Protein expression of p-p38 MAPK detected via WB.

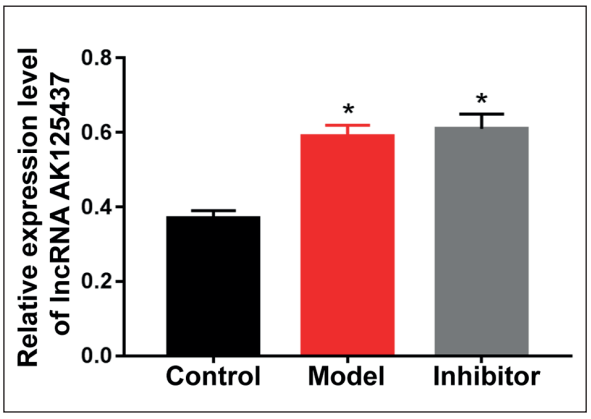

Figure 6. Relative expression level of lncRNA AK125437 in each group. Note: *p<0.05 *vs.* normal group.

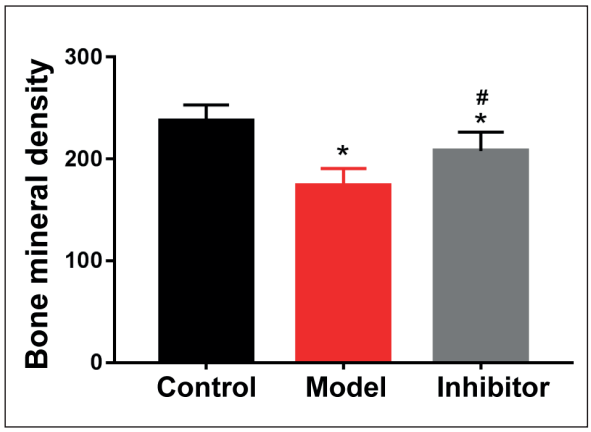

Figure 8. Bone mineral density in each group. Note: *p<0.05 *vs.* normal group, and #p<0.05 *vs.* model group.

It will even influence cardiopulmonary function in severe cases. In particular, postmenopausal osteoporosis-induced fracture and malformation cause patients to lie in bed for a long term. This seriously affects the life quality of patients and even result in death. MAPK signaling pathway is an important cell signal transduction pathway. Currently, it is recognized that the pathway bears close relation with bone metabolism, as well as bone formation and destruction. Meanwhile, it is involved in regulating the proliferation and differentiation of osteoclasts[11,12]. In this pathway, p38 MAPK is a critical molecule. Stimulated by various factors and cytokines, p38 MAPK can be activated by a large number of inflammatory factors released by damaged tissues and cells. This promotes its phosphorylation and forms p-p38 MAPK that can enter the nucleus to activate multiple transcriptional factors[13,14]. Particularly, after the onset of postmenopausal osteoporosis, under the stimulation by estrogen insufficiency, RANKL synthesized and secreted in bone tissues can bind to that on the surface of undifferentiated osteoclasts to phosphorylate p38 MAPK and form p-p38 MAPK. Ultimately, this may activate the MAPK signaling pathway in undifferentiated osteoclasts, which also enables them to differentiate into mature ones. As a result, osteoporosis is induced due to a worsened bone loss[15,16].

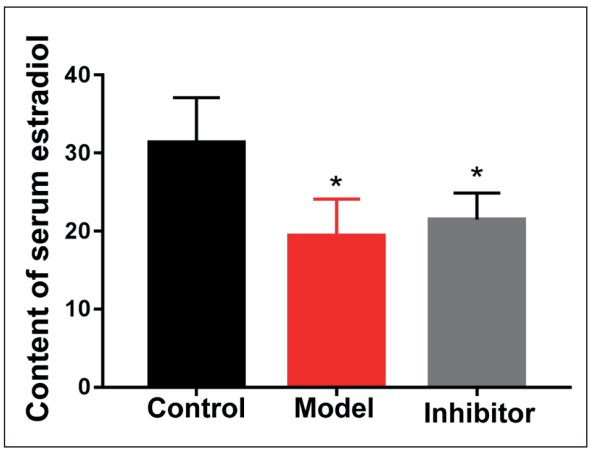

Figure 7. Content of serum estradiol. Note: *p<0.05 *vs.* normal group.

In the present research, we revealed that bone mineral density was substantially lower in ovariectomized rats than normal rats. This suggested that ovariectomized female rats might suffer from postmenopausal osteoporosis indeed. At the same time, RANKL and p-p38 were abnormally highly expressed in bone tissues of ovariectomized rats. Meanwhile, they were notably higher than those in normal group, indicating that the MAPK signaling pathway was activated in bone tissues of postmenopausal osteoporosis model rats.

LncRNAs, as a class of RNAs with more than 20 nucleotides in length, can regulate gene expression with no protein-encoding function[17,18]. LncRNAs play important regulatory roles in major physiological and pathological processes, such as cell development, proliferation, differentiation, survival, and apoptosis. Moreover, they can modulate downstream miRNAs to regulate several cellular signaling pathways, thereby affecting the regulations at epigenetic, transcriptional, and post-transcriptional levels[19,20]. As an important lncRNA, lncRNA AK125437 can regulate various signaling pathways. It has also been confirmed to participate in the occurrence and development

of bone metabolism-related diseases by regulating several signaling pathways. In this study, we found that the relative expression level of lncRNA AK125437 was substantially up-regulated in bone tissues of postmenopausal osteoporosis model rats. This suggested that lncRNA AK125437 was involved in the onset of postmenopausal osteoporosis, which was also closely associated with the decreased the bone mineral density of model rats. Meanwhile, in postmenopausal osteoporosis model rats, the MAPK signaling pathway was aberrantly activated in bone tissues. MAPK signaling pathway inhibitor could notably down-regulate the expressions of RANKL and p-p38 MAPK, thereby suppressing the MAPK signaling pathway. Eventually, this mitigated osteoporosis and increased the bone mineral density, without changing the expression of lncRNA AK125437. Therefore, it could be concluded that lncRNA AK125437 influenced the bone mineral density of rats with postmenopausal osteoporosis by activating the MAPK pathway.

Conclusions

We first revealed that lncRNA AK125437 influences bone mineral density of rats with postmenopausal osteoporosis by activating the MAPK pathway.

Conflict of Interests

The Authors declare that they have no conflict of interests.

References

1) Wang Q, Li Y, Zhang Y, Ma L, Lin L, Meng J, Jiang L, Wang L, Zhou P, Zhang Y. LncRNA MEG3 inhibited osteogenic differentiation of bone marrow mesenchymal stem cells from postmenopausal osteoporosis by targeting miR-133a-3p. Biomed Pharmacother 2017; 89: 1178-1186.
2) Yeh Y, Slovik D, Carter D, Clapp M, Churchill W, Reddy P. Intravenous bisphosphonates for post-menopausal osteoporosis: adherence to a network guideline. J Clin Pharm Ther 2011; 36: 342-347.
3) Paschalis EP, Gamsjaeger S, Hassler N, Fahrleitner-Pammer A, Dobnig H, Stepan JJ, Pavo I, Eriksen EF, Klaushofer K. Vitamin D and calcium supplementation for three years in postmenopausal osteoporosis significantly alters bone mineral and organic matrix quality. Bone 2017; 95: 41-46.
4) Mignot MA, Taisne N, Legroux I, Cortet B, Paccou J. Bisphosphonate drug holidays in postmenopausal osteoporosis: effect on clinical fracture risk. Osteoporos Int 2017; 28: 3431-3438.
5) Liu Q, Huang J, Zhou N, Zhang Z, Zhang A, Lu Z, Wu F, Mo YY. LncRNA loc285194 is a p53-regulated tumor suppressor. Nucleic Acids Res 2013; 41: 4976-4987.
6) Chen G, Wang Z, Wang D, Qiu C, Liu M, Chen X, Zhang Q, Yan G, Cui Q. LncRNADisease: a database for long-non-coding RNA-associated diseases. Nucleic Acids Res 2013; 41: D983-D986.
7) Niu C, Yuan K, Ma R, Gao L, Jiang W, Hu X, Lin W, Zhang X, Huang Z. Gold nanoparticles promote osteogenic differentiation of human periodontal ligament stem cells via the p38 MAPK signaling pathway. Mol Med Rep 2017; 16: 4879-4886.
8) Feng YL, Yin YX, Ding J, Yuan H, Yang L, Xu JJ, Hu LQ. Alpha-1-antitrypsin suppresses oxidative stress in preeclampsia by inhibiting the p38MAPK signaling pathway: an in vivo and in vitro study. PloS One 2017; 12: e173711.
9) Li W, Zhu HM, Xu HD, Zhang B, Huang SM. CRNDE impacts the proliferation of osteoclast by estrogen deficiency in postmenopausal osteoporosis. Eur Rev Med Pharmacol Sci 2018; 22: 5815-5821.
10) Cano A, Chedraui P, Goulis DG, Lopes P, Mishra G, Mueck A, Senturk LM, Simoncini T, Stevenson JC, Stute P, Tuomikoski P, Rees M, Lambrinoudaki I. Calcium in the prevention of postmenopausal osteoporosis: EMAS clinical guide. Maturitas 2018; 107: 7-12.
11) Sato K, Shirai R, Yamaguchi M, Yamashita T, Shibata K, Okano T, Mori Y, Matsuyama TA, Ishibashi-Ueda H, Hirano T, Watanabe T. Anti-atherogenic effects of vaspin on human aortic smooth muscle cell/macrophage responses and hyperlipidemic mouse plaque phenotype. Int J Mol Sci 2018; 19:
12) Kim MY, Ilyosbek S, Lee BH, Yi KY, Jung YS. A novel urotensin II receptor antagonist, KR-36676, prevents ABCA1 repression via ERK/IL-1beta pathway. Eur J Pharmacol 2017; 803: 174-178.
13) Giovannini MG, Scali C, Prosperi C, Bellucci A, Vannucchi MG, Rosi S, Pepeu G, Casamenti F. Beta-amyloid-induced inflammation and cholinergic hypofunction in the rat brain in vivo: involvement of the p38MAPK pathway. Neurobiol Dis 2002; 11: 257-274.
14) Feng D, Ling WH, Duan RD. Lycopene suppresses LPS-induced NO and IL-6 production by inhibiting the activation of ERK, p38MAPK, and NF-kappaB in macrophages. Inflamm Res 2010; 59: 115-121.
15) Yamashita M, Otsuka F, Mukai T, Yamanaka R, Otani H, Matsumoto Y, Nakamura E, Takano M, Sada KE, Makino H. Simvastatin inhibits osteoclast differentiation induced by bone morphogenetic protein-2 and RANKL through regulating MAPK, AKT and Src signaling. Regul Pept 2010; 162: 99-108.
16) Siddiqi MH, Siddiqi MZ, Kang S, Noh HY, Ahn S, Simu SY, Aziz MA, Sathishkumar N, Jimenez PZ, Yang DC.

Inhibition of osteoclast differentiation by ginsenoside Rg3 in RAW264.7 cells via RANKL, JNK and p38 MAPK pathways through a modulation of cathepsin K: an in silico and in vitro study. Phytother Res 2015; 29: 1286-1294.

17) Chen G, Wang Z, Wang D, Qiu C, Liu M, Chen X, Zhang Q, Yan G, Cui Q. LncRNADisease: a database for long-non-coding RNA-associated diseases. Nucleic Acids Res 2013; 41: D983-D986.

18) Crea F, Watahiki A, Quagliata L, Xue H, Pikor L, Parolia A, Wang Y, Lin D, Lam WL, Farrar WL, Isogai T, Morant R, Castori-Eppenberger S, Chi KN, Wang Y, Helgason CD. Identification of a long non-coding RNA as a novel biomarker and potential therapeutic target for metastatic prostate cancer. Oncotarget 2014; 5: 764-774.

19) Zhou M, Wang X, Li J, Hao D, Wang Z, Shi H, Han L, Zhou H, Sun J. Prioritizing candidate disease-related long non-coding RNAs by walking on the heterogeneous lncRNA and disease network. Mol Biosyst 2015; 11: 760-769.

20) Li A, Ge M, Zhang Y, Peng C, Wang M. Predicting long noncoding RNA and protein interactions using heterogeneous network model. Biomed Res Int 2015; 2015: 671950.